Geomorphology 190 (2013) 73–81

Contents lists available at SciVerse ScienceDirect

Geomorphology

journal homepage: www.elsevier.com/locate/geomorph

Landslide model performance in a high resolution small-scale landscape

V. De Sy [a,b,*], J.M. Schoorl [a], S.D. Keesstra [b], K.E. Jones [c], L. Claessens [a,d]

[a] Soil Geography and Landscape group, Wageningen University, P.O. Box 47, 6700 AA Wageningen, The Netherlands
[b] Soil Physics and Land Management Group, Wageningen University, P.O. Box 47, 6700 AA Wageningen, The Netherlands
[c] School of Geography, Environment and Earth Sciences, Victoria University of Wellington, Wellington, Wellington 6012, New Zealand
[d] International Crops Research Institute for the Semi-Arid Tropics (ICRISAT), P.O. Box 39063, 00623 Nairobi, Kenya

ARTICLE INFO

Article history:
Received 30 May 2012
Received in revised form 28 January 2013
Accepted 18 February 2013
Available online 26 February 2013

Keywords:
Landslide locations
LAPSUS-LS
New Zealand
DEM resolution
Model performance

ABSTRACT

The frequency and severity of shallow landslides in New Zealand threatens life and property, both on- and off-site. The physically-based shallow landslide model LAPSUS-LS is tested for its performance in simulating shallow landslide locations induced by a high intensity rain event in a small-scale landscape. Furthermore, the effect of high resolution digital elevation models on the performance was tested. The performance of the model was optimised by calibrating different parameter values. A satisfactory result was achieved with a high resolution (1 m) DEM. Landslides, however, were generally predicted lower on the slope than mapped erosion scars. This discrepancy could be due to i) inaccuracies in the DEM or in other model input data such as soil strength properties; ii) relevant processes for this environmental context that are not included in the model; or iii) the limited validity of the infinite length assumption in the infinite slope stability model embedded in the LAPSUS-LS. The trade-off between a correct prediction of landslides versus stable cells becomes increasingly worse with coarser resolutions; and model performance decreases mainly due to altering slope characteristics. The optimal parameter combinations differ per resolution. In this environmental context the 1 m resolution topography resembles actual topography most closely and landslide locations are better distinguished from stable areas than for coarser resolutions. More gain in model performance could be achieved by adding landslide process complexities and parameter heterogeneity of the catchment.

1. Introduction

Landslides triggered by rainstorms present a global environmental and economic hazard, especially on steep hillslopes in populated areas. In mountainous countries, such as New Zealand, shallow landsliding is one of the most important erosion processes (Crozier, 1986). The frequency and severity of shallow landslides threaten life and property, both on- and off-site (Brooks et al., 2002; Reid and Page, 2002). A long-term consequence is the loss of soil nutrients, and as a result a decline in soil productivity. Pasture production on 20-year old landslide scars can be as low as 20% compared to unaffected areas (Trustrum et al., 1984; in Brooks et al., 2002). In order to effectively battle the on- and off-site effects of landslides, more information is needed on the spatial distribution of potential landslide hazard in the landscape and the associated possible contribution to catchment sediment load.

Numerous landslide models have been developed to predict spatially explicit landslide hazard to mitigate unwanted effects. Most recent models combine steady-state hydrology concepts with the infinite slope stability model to estimate critical rainfall, which is the steady-state rainfall threshold to cause slope failure (e.g. Montgomery and Dietrich, 1994; Borga et al., 1998; Burton and Bathurst, 1998; Claessens et al., 2005). One of the main factors determining the landslide location is surface topography through concentration of shallow subsurface flow and increased soil saturation which can trigger slope failure (Borga et al., 2002a). Other important input parameters are rainfall intensity, geomorphological expression (gradients and topography), and soil and vegetation properties. These types of data might be difficult to gather, especially over large and complex landscapes.

Resolution of a digital elevation model (DEM) influences the calculation of critical rainfall (Zhang and Montgomery, 1994; Claessens et al., 2005), through derivation of topographical and hydrological parameters, and therefore the prediction of landslide locations. Moreover, in the last few years there is an emergence of promising new technologies for high resolution terrain mapping (e.g. total stations, terrestrial laser scanners and LiDAR). High resolution digital elevation data recognise more local variations in hillslope and valley morphology and thus might increase the potential in the detailed analysis of landslide locations (Tarolli and Fontana, 2009). However, Zhang and Montgomery (1994) suggest that a grid size of 10 m would suffice for DEM-based geomorphic and hydrological modelling. Tarolli and Tarboton (2006) noticed that a very high resolution DEM may lower performance of an

* Corresponding author at: Soil Geography and Landscape group, Wageningen University, P.O. Box 47, 6700 AA Wageningen, The Netherlands. Tel.: +31 317 48 19 15.
E-mail address: niki.desy@wur.nl (V. De Sy).

0169-555X/$ – see front matter © 2013 Elsevier B.V. All rights reserved.
http://dx.doi.org/10.1016/j.geomorph.2013.02.012

infinite slope stability model. The surface topography at this resolution might be less representative of the more general slope conditions under which landslides occur. Given the advances in high quality digital elevation data, it is desirable to investigate their effect on the performance of landslide models.

Claessens et al. (2005) developed the LAPSUS-LS model to predict landscape evolution due to landslides on coarse temporal and spatial scales, with limited data requirements. Often there is a lack of representative and detailed soil-mechanical and hydrological parameters which might constrain models aiming for event-based landslide prediction on finer spatial and temporal scales. This study tests the LAPSUS-LS model beyond its original scope to explore its performance in predicting the spatial distribution of landslides, without the need for detailed spatially explicit input data, when calibrated and validated with high resolution elevation data for a small scale catchment in New Zealand. This study additionally investigates the impact of finer resolution digital topography on simulated landslides.

2. Regional setting

2.1. Study area

Due to data availability, including a storm and landslide inventory, we applied the landslide model LAPSUS-LS (LandscApe ProcesS modelling at mUlti dimensions and scaleS with a LandSlide component) to a small catchment (0.1 km^2) in New Zealand to assess model performance in small-scale landscapes with a high resolution (<10 m) DEM. The Hinenui study area is located in the coastal hills south-east of Gisborne on the eastern side of North Island, New Zealand (Fig. 1). The geology of the area predominantly consists of Miocene undifferentiated massive and bedded, slightly calcareous mudstone (Mazengarb and Speden, 2000). The study catchment consists of two small valleys which merge into a common floodplain. The catchment contains no permanent channels but evidence of ephemeral channels is present, which function during intense rainfall events (Preston, 2008; Jones, 2009). The elevation ranges from 22.9 to 178.7 m a.s.l., while having an average slope of 23.3°. Most of the watershed is covered with pasture, with a few scattered trees.

Average annual rainfall in the region ranges from about 1000 mm on the coast near Gisborne to 2500 mm further inland. A large part, about 45%, of the annual precipitation falls during the winter months (May–August). The winter storms are usually of low intensity and long duration. However, from March to May, tropical cyclones occasionally cause high-intensity, short-duration storms. In addition, localised, brief high-intensity convective storms can occur in the area. All these types of storms are able to trigger landslides in the study area (Reid and Page, 2002).

2.2. Storm event August 2002

From August 5th to 7th 2002, the East Coast and northern Hawke´s bay were struck by a high-intensity rainfall storm. Near Gisborne, the highest rainfall recorded was over 300 mm for the entire event. Local

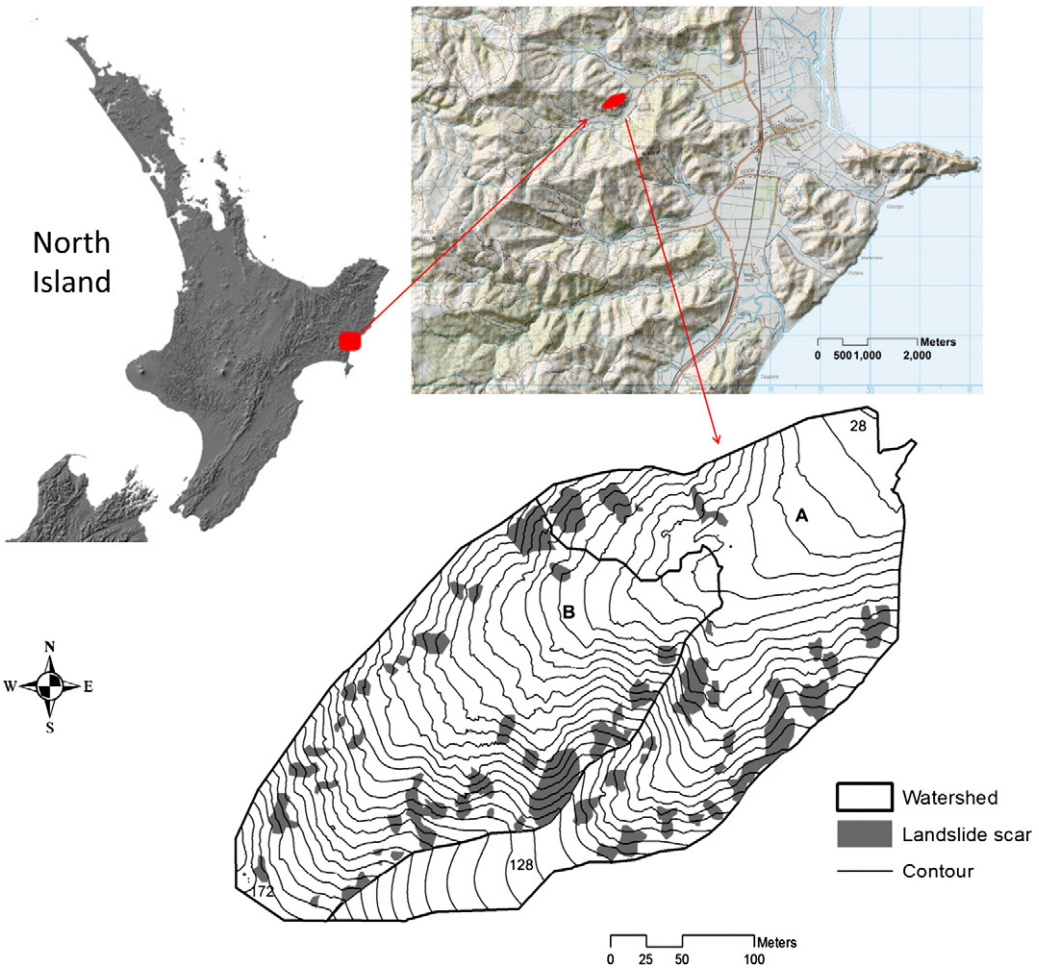

Fig. 1. DEM of the study area (contour interval 4 m) showing observed locations of landslide scars in A) calibration and B) validation catchment.

landowners reported that most of the landsliding occurred towards the end of the storm following 12 hours of high-intensity precipitation (Preston, 2008). Rainfall data for the Hinenui study area for the August 2002 event was obtained through the National Climate Database of New Zealand. Daily rainfall data from four virtual climate stations (VCS) in the vicinity of the Hinenui catchment show an average rainfall of 104.4 mm day^{-1} on August 6th (Table 1). VCS data are estimates of daily rainfall on a regular (~5 km) grid based on the spatial interpolation of actual data observations made at climate stations located around the country. A thin-plate smoothing spline model was used for the spatial interpolations (http://cliflo.niwa.co.nz).

3. Materials and methods

3.1. Modelling framework

This study used the LAPSUS modelling framework. LAPSUS is a multi-dimensional landscape evolution model addressing on-site and off-site effects of current and possible future water and soil redistribution by water run-off and tillage erosion (Schoorl et al., 2000). Claessens et al. (2005, 2007a,b) extended the model with a landslide component (LAPSUS-LS), which is able to model the triggering of shallow landslides as a function of critical rainfall, their subsequent trajectory downwards and the final deposition of the lobe with sediment delivery rates to streams (Claessens et al., 2006).

3.2. Critical rainfall

The calculation of critical rainfall is based on a steady-state hydrological model in combination with a deterministic infinite slope stability model to delineate areas prone to landsliding due to surface topographic effects on hydrologic response (Montgomery and Dietrich, 1994; Pack et al., 2001; Claessens et al., 2007a,b). In an infinite slope stability model, the stability of a slope is usually expressed as the factor of safety (*FS*), which can be written as (Pack et al., 2001; Claessens et al., 2007a,b):

$$FS = \frac{C + \cos\theta\left[1 - W\left(\frac{\rho_w}{\rho_s}\right)\right]\tan\phi}{\sin\theta} \quad (1)$$

where C is the combined cohesion made dimensionless relative to the perpendicular soil thickness (−), θ local slope angle (°), W the relative wetness index (−), ρ_w density of water (g cm^{-3}), ρ_s wet soil bulk density (g cm^{-3}) and φ the angle of internal friction of the soil (°).

If *FS* is larger than 1, the slope is stable; if *FS* is below 1, the slope becomes unstable and a landslide will be triggered on that position. C can be interpreted as the relative contribution to slope stability of the cohesive forces, which consist of root cohesion and soil cohesion (Claessens et al., 2007a,b). W is the ratio of local flux at a given steady-state rainfall to that at soil profile saturation. Claessens et al. (2007a,b) used a steady-state hydrological response model based on work by O'Loughlin (1986) and Moore et al. (1988) for the calculation of W:

$$W = \frac{Ra}{bT\sin\theta} \quad (2)$$

where R is steady-state rainfall recharge (m d^{-1}), a the upslope contributing drainage area (m^2), b the grid size (m), T soil transmissivity when saturated (m^2 day^{-1}) and θ the local slope angle (°).

The upslope contributing area is calculated using the concept of multiple downslope flow (Quinn et al., 1991). Wetness ranges between 0 and 1, since any excess of water is assumed to form overland flow.

By substituting Eq. (2) into Eq. (1), equating *FS* to 1 since this is the threshold for instability, and solving for R, the minimum steady-state rainfall to cause slope failure, termed critical rainfall Q_{cr} (m d^{-1}), can be determined as (Claessens et al., 2007a,b):

$$Q_{cr} = T\sin\theta\left(\frac{b}{a}\right)\left(\frac{\rho_s}{\rho_w}\right)\left[1 - \frac{(\sin\theta - C)}{(\cos\theta\tan\phi]}\right. \quad (3)$$

With the boundary conditions for W (between 0 and 1), the upper and lower thresholds for slopes that can fail can be calculated with Eq. (3). Unconditionally stable areas are predicted to be stable, even when saturated and satisfy the following condition (Claessens et al., 2007a,b):

$$\tan\theta \leq \left(\frac{C}{\cos\theta}\right) + \left(1 - \frac{\rho_w}{\rho_s}\right)\tan\phi \quad (4)$$

Unconditionally unstable areas, consisting mostly of bedrock outcrops and unstable even when dry, satisfy the following condition (Claessens et al., 2007a,b):

$$\tan\theta > \tan\phi + \left(\frac{C}{\cos\theta}\right). \quad (5)$$

3.3. Trajectories of failed slope material

When the amount of rainfall exceeds the critical rainfall in a grid cell, the landslide starts and debris begins moving downslope. Following the initial failure, unstable soil material is eroded. The depth of such material (S, in m) can be estimated based on works by Johnson and Rodine (1984, as in Claessens et al., 2007a) and e.g. Burton and Bathurst (1998) as:

$$S = \frac{\rho_s\cos(\tan\theta - \tan\alpha)\cdot\delta}{C_s} \quad (6)$$

where α is the minimum local slope for debris flow movement (°), δ a correction factor for dimensions (m^2) and C_s is soil cohesion (kPa).

Landslide erosion follows the steepest descent and stops where the gradient falls below a certain slope angle α and the transported material is deposited over a number of downslope grid cells, defined as 'cell distance' D (−):

$$D = \frac{r}{b} \quad (7)$$

where r is the run out distance (m), and b grid size or DEM resolution (m). Here, r of the depositional phase defines the distance over which material will be deposited and is calculated using the following equation from Burton and Bathurst (1998):

$$r = \chi\cdot\ \Delta y \quad (8)$$

Table 1
Virtual climate station data: 24-h rainfall total (mm) from 9 AM on August 6th, 2002.

Station number	Rain (mm d^{-1})
28027	80.0
29601	94.9
30100	131.6
30637	111.1

Source: http://cliflo.niwa.co.nz.

where Δy stands for the elevation difference between the head of the slide and the point where deposition begins (m), and χ an empirically derived fraction set at 0.4 (−).

The accumulated soil material is then further routed with 'double' multiple flow methodology (Quinn et al., 1991; Claessens et al., 2005, 2007a) to downslope neighbours until $D < 1$, where all the remaining sediment is deposited and the landslide halts (Claessens et al., 2007a). The sediment which is effectively delivered to grid cell n (S_n) is expressed as:

$$S_n = \left(\frac{B_{n-1}}{D_{n-1}}\right) f_n. \tag{9}$$

The term B_{n-1}/D_{n-1} is the amount of sediment deposited in the grid cell n, originating from erosion upslope, divided by cell-distance (see Eq. (7)). The fraction allocated to each lower neighbour is represented and determined by the multiple flow concept described by Quinn et al. (1991). The remaining sediment budget of the grid cell n which is not deposited but 'passed through' to the grid cell $n + 1$ can be written as:

$$B_n = B_{n-1}\left(1 - \frac{1}{D_{n-1}}\right) f_n. \tag{10}$$

3.4. DEM and map preparation

This study used a 1 m resolution digital elevation model (DEM), obtained in April 2008 by terrestrial laser scanning (Jones, 2009). The sinks in the DEM were filled, after which flats and pseudo-flats were removed to ensure that the LAPSUS-LS works with full hydrological connectivity and properly calculated upslope contributing areas. To investigate the influence of modelling resolution on the model performance, DEMs with 2, 5 and 10 m cell sizes were aggregated from the 1 m DEM.

Preston (2008) identified 71 earth flow failures at the study site within days of the storm event described above. The 71 scars at the study site were identifiable on a low resolution 2002 aerial photo taken immediately after the storm event which clearly shows landslide scars and debris tails. From this aerial photograph a vector polygon layer map of the landslide scars was created (Jones, 2009). The polygon layer was also rectified against a high resolution ortho-rectified aerial photograph from 2007 and checked against field mapping of visible scars in 2008. Only one land cover class, pasture, was considered for both the calibration and validation catchments.

3.5. Input parameters

The default settings for the empirical parameters used in the soil redistribution equations (Eqs. (6) to (10)) were taken from Claessens et al. (2007a). The run-out fraction χ (Eq. (8)) was set to 0.4 and the minimum slope angle for maintaining flow α was set to 10°. Regolith depth (h) and soil cohesion (C_s) were set to a constant value, respectively 1 m and 10 kPa. These settings are based on field evidence and literature (Burton and Bathurst, 1998; Claessens et al., 2006, 2007a).

3.6. Testing model performance

To asses model performance it is important to evaluate the prediction of stable as well as unstable cells. If model performance is only based on the ratio of successfully predicted landslide sites over total actual landslide sites, over-prediction of landslides is not accounted for. Therefore, a measure that indicates the model performance in prediction of stable as well as unstable cells is preferred. Keijsers et al. (2011) used the modified success rate (*MSR*), proposed by Huang and Kao (2006), to asses LAPSUS-LS performance in predicting landslide locations in Taiwan. *MSR* is calculated as follows:

$$MSR = 0.5 \times \frac{CPP}{NMP} + 0.5\frac{PSC}{NSC} \tag{11}$$

with *CPP* the number of landslide polygons that are correctly predicted, *NMP* total number of mapped landslide polygons, *PSC* number of correctly predicted stable cells and *NSC* total number of actual stable cells.

A landslide polygon is considered correctly predicted if at least one cell with predicted erosion occurs within its boundary. A stable cell is counted as correctly predicted if it is not predicted as landslide erosion or deposition and is not contained in a landslide polygon. *MSR* can range from 0 to 1. If all cells are classified as stable or all cells are classified as landslides, *MSR* is 0.5. The highest score of 1 is achieved when both the landslide polygons and stable cells are perfectly predicted.

3.7. Calibration and validation procedure

MSR was used to optimise the prediction of landslide locations by the LAPSUS-LS for the August 2002 event. The values for ρ_s, C, T and φ and critical rainfall threshold were used as calibration parameters. The critical rainfall threshold for landslide initiation is usually a fixed parameter, with values estimated from precipitation data. However, the model interprets the critical rainfall threshold value as a steady-state rainfall which might not account for variations in intensity during the rainfall event. Furthermore, not all precipitation actually contributes to sub-surface flow e.g. because of interception by vegetation. As such, this parameter can also be used to optimise model performance. *MSR* for the calibration catchment was calculated for a range of parameter values and increments (see Table 2) to find the best model fit for 1, 2, 5 and 10 m resolutions. The optimal parameters were then applied to the validation catchment (1 m resolution).

4. Results and discussion

4.1. Model performance at 1 m resolution

The 1 m resolution DEM was used for the optimisation runs with the indicated value ranges and increments of the optimisation parameters (Table 3). The optimal *MSR* value for the calibration catchment is 0.851. The model is able to correctly predict 89.7% of landslide locations and 80.6% of stable cell areas. Applying the same parameter combination to the validation catchment results in an *MSR* value of 0.648.

Visual analysis of landslide locations (Fig. 2) shows that landslides higher up the slope, near the water divide are under-predicted and that there is an over-prediction of landslide trajectories where the water converges on the slope (e.g. valley bottom and drainage channels).

Difference in the calibration and validation model performances could be due to different morphologic or soil characteristics of the two small catchments which make different parameter combinations

Table 2
Range and increments of optimisation parameters for calibration.

Parameter	Range	Increment
Bulk density ρ_s (g cm^{-3})	1.4–1.8	0.1
Combined cohesion C (−)	0.1–0.4	0.1
Angle of internal friction φ (°)	28.4–36.4	1
Transmissivity T (m^2 d^{-1})	10–18	1
Critical rainfall threshold (m d^{-1})	0.01–0.1	0.01

Table 3
Model performance *MSR* for the calibration and validation catchments, including landslide and stable cell prediction and optimal parameter combinations.

	MSR (−)	Landslide prediction	Stable cell prediction	*C* (−)	φ (°)	*T* ($m^2\ d^{-1}$)	ρ_s ($g\ cm^{-3}$)	Critical rainfall threshold ($m\ d^{-1}$)
Calibration	0.851	0.897	0.806	0.1	30.4	15	1.8	0.01
Validation	0.648	0.725	0.570					

more suitable for each catchment. However, even with optimised parameter values, the maximum *MSR* value for the validation catchment is only 0.707.

The model performance for the entire range of *C*, *T*, ρ_s and φ, with the critical rainfall threshold set to 0.01 m d^{-1}, is plotted for the calibration and validation catchments (Fig. 3). For both catchments there is a trade-off between a good prediction of landslide sites and that of stable cells, as can be seen from the dome-shape of the plotted success rates. Furthermore these plots show that this trade-off is more severe for the validation catchment, resulting in a lower *MSR* value.

In Fig. 4 the critical rainfall values are presented for both catchments. For the validation catchment landslides are more over-predicted (lower *MSR* for stable cell prediction), because slopes are still steep enough to cause landslides where the water converges. In the calibration catchment the slopes are generally much more gentle, where the water converges, proven by the larger area that is unconditionally stable (Fig. 4).

In the following sections we argue that the inaccuracy in predicting landslide locations could be due to i) the exclusion, from the model, of relevant processes causing landslides in this specific context (Borga et al., 1998); ii) incorrect or incomplete input data such as inaccuracies in the DEM and spatial variability in soil and vegetation related parameters; or iii) the reduced validity of the infinite length assumption in the infinite slope stability model for high resolution DEMs and landslides with small length/depth ratios.

4.1.1. Exclusion of relevant processes

There are several processes that are not represented in the LAPSUS-LS model that might have an influence on the triggering of landslides: i) regolith stripping, ii) preferential flow paths, and iii) non steady-state hydrological processes.

Brooks et al. (2002) described the process of regolith stripping in the Hawke's Bay region with three significant phases based on Crozier and Preston (1999). The stripping of the regolith layer progressively moves upslope with subsequent landslide events and landslide debris deposited at the base of the slope (Crozier and Preston, 1999; Brooks et al., 2002). Preston (2008) describes the specific geometry of the Hinenui catchment as a mosaic of old failure scars and associated colluvial deposits on middle and lower slopes, while the remnant of undisturbed regolith can mainly be found on the spurs and crests of slopes. Landslide debris deposited downslope frequently shows an increase in bulk density, internal friction angle and cohesion, increasing the resistance to failure (Preston, 1996; Crozier and Preston, 1999; Brooks et al., 2002). In contrast, the increase in regolith depths downslope may decrease resistance to failure, by the development of higher pore water pressures. However, in combination with lower slope angles, the overall result for the colluvial foot slope is likely one of higher stability. More uphill, removal of failed landslide material could take away support and may trigger upslope failure (see Claessens et al., 2007a). This means that the trigger locations of landslides might be correctly predicted by the model but as it does not include the parameterisation of the above mentioned processes, upslope failures are not always accurately predicted.

Changes in both the hydrological and geotechnical conditions of the slope add more complexity to the calculation of critical rainfall values as they change thresholds for slope failure. Therefore, landslide predictions might be more accurate when changes in both the hydrological and geotechnical properties, as regolith develops on slopes, are taken into account. This concept of different phases of regolith stripping introduces the importance of the legacy effect of landsliding on the landscape, and especially on the DEM for modelling purposes

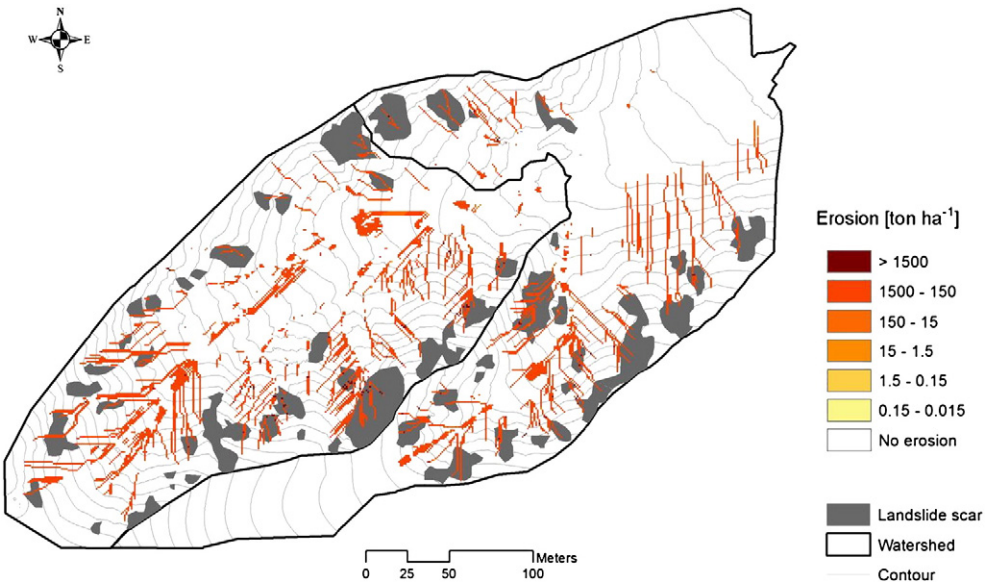

Fig. 2. Example of modelling landslide locations and trajectories at 1 m resolution.

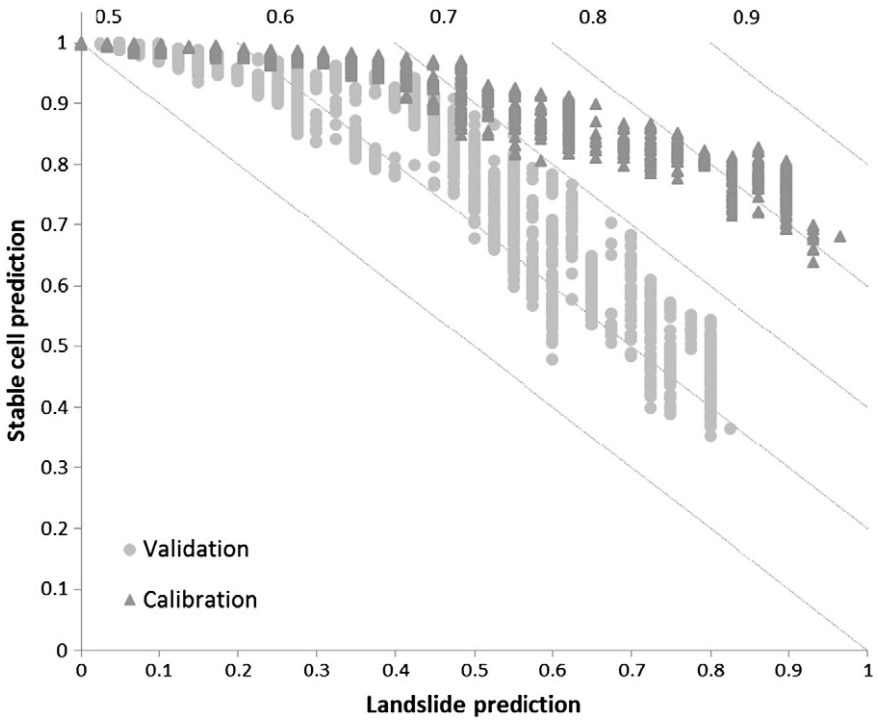

Fig. 3. Model performance during parameter optimisation. All model runs are shown for both the calibration and validation catchments. *MSR* is indicated as diagonals.

(Hewitt et al., 2008, Keijsers et al.2011). The prediction of landslide locations might improve by modelling the storm in multiple time steps and by introducing spatial heterogeneity of soil strength parameters in the model.

Another process not represented in the current model is preferential flow paths of throughflow such as piping. Preston (2008) stated that in some cases sub-surface flow in pipes was identified as a factor in triggering landslides in the Hinenui catchment. The occurrence of sub-surface flow could be, among others, caused by sub-horizontal bedded parent material. Natural pipes or other macropores can carry significant downslope flows and act as a bypass to soil flow (Borga et al., 1998). These processes are not included in the LAPSUS-LS model, but will likely influence the triggering of landslides. However, there are at present many difficulties and uncertainties in pipe flow modelling (Jones, 2010).

The assumption of steady-state hydrology as well as steady-state rainfall characteristics might lead to inaccurate prediction of landslides for this study area. The assumption of steady-state hydrology implies that the relative potential for shallow landslides is determined by convergence of shallow subsurface flow, determined by

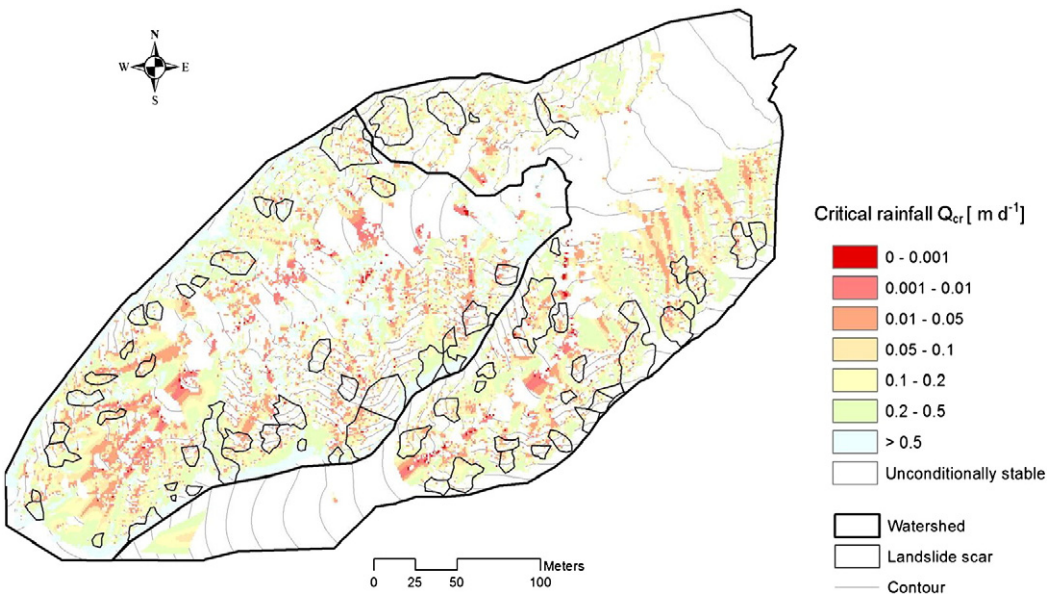

Fig. 4. Map of critical rainfall values for landslide initiation for the Hinenui catchment.

surface topography, and is proportional to the upslope contributing area (Montgomery and Dietrich, 1994; Claessens et al., 2007a). The low velocity of subsurface flow might indicate that most areas in the catchment do not receive subsurface flow from their entire upslope contributing area (Borga et al., 2002a). Furthermore, the steady-state hydrology assumption might not be valid for high-intensity rains (Iverson, 2000). Chiang and Chang (2009) reported that the steady-state assumption results in less accurate prediction of landslides with a small contributing area, as is the case for most landslides in our catchment. Assuming steady-state hydrology also does not take into account the hydrological processes acting on the initially unsaturated soil and its initial wetness conditions. Several studies introduce a quasi-dynamic wetness index as an alternative approach to overcome some limitations of the steady-state assumption (e.g. Barling et al., 1994; Borga et al., 2002b).

In addition to these three most important processes, landslide initiation might also be influenced by soil heterogeneity, variations in vegetation density and spatial distribution of rainfall which are presently not accounted for in the model. However, while extending the model with more detailed data and processes might improve model performance, they demand more detailed information on triggering rainfall events and soil properties than is usually available or feasible to collect.

4.1.2. Incorrect or incomplete input data

A second type of error is incomplete or incorrect input data. Given that topography is one of the main drivers of slope failure, the quality of the DEM is important. Elevation values are used to calculate surface derivatives such as slope, aspect, flow direction, catchment boundaries and upstream contributing area. As already mentioned, the DEM was processed several years after the 2002 rainfall event. Consequently, alteration of the surface and topography after the landslide event might indirectly be included. On the other hand, given the legacy effect of landslides in this landscape, old landslide scars were most likely already present before the event, justifying the use of the 2008 DEM.

In the calculation of *MSR* a stable cell or a landslide cell is defined by respectively the absence or the occurrence of erosion, including the slide trajectory, as well as deposition in that cell. In the observed landslide polygon layer only the visible landslide erosion scar was included, often light coloured as a result of the bedrock or saprolite exposure. The sediment debris path and deposition lobe with dark coloured soil material were often not mapped. This will likely influence the calculation of *MSR*. These darker sediment lobes, usually present in the drainage ways might obscure erosion scars. Therefore, part of the over-prediction of landslides in these locations might not be due to model inaccuracy but because of inaccuracy in landslide mapping.

Spatial heterogeneity of soil and vegetation characteristics was not taken into account in our modelling. Lumping of soil and vegetation parameters could influence model performance by ignoring important spatial variability, and related processes, in the landscape. Finally, no field data were available for estimation of soil parameters. The parameter values used for modelling were chosen because they best fit the model equations, but it is not clear if they have a valid link with the physical reality.

4.1.3. Limited validity of the infinite length assumption

Milledge et al. (2012) have shown that the infinite length assumption within the infinite slope stability model is only valid for landslides with a high length/depth (L/H) ratio. They established a critical L/H ratio of 25, implying reasonable validity of the assumption for modelling when a coarse (>25 m) DEM resolution is used. For models with a finer resolution (<10 m) DEM, the assumption of infinite length proves to be less valid depending on the assumed landslide failure plane depth and on the material properties. In our study area, most landslides have an L/H ratio >25 (see Fig. 1, typical landslide depth is 1 m). However, as also found by Milledge et al. (2012), the limited validity of the assumption could be responsible for the under-prediction of landslides upslope, which in general have a somewhat smaller L/H ratio. Milledge et al. (2012) also conclude that the infinite length assumption can be valid for smaller DEM resolutions (e.g., 1 m). Lateral subsurface flow determines pore water pressure in our study area; the spatial organisation in the predicted pore water pressure field reduces the probability of short landslides; and minimises the risk that predicted landslides will have L/H ratios less than 25.

4.2. Influence of DEM resolution

Apart from the process type errors in the model outputs, we also assessed the model performance for the entire range of optimisation parameters for the calibration catchment, with 1, 2, 5 and 10 m resolution DEMs. There is a clear decrease in model performance with coarser DEM resolutions (Table 4), illustrating the fact that it is increasingly difficult for the model to predict accurate landslide patterns.

The optimal combination of parameters differs for each DEM resolution. Only for the optimised rainfall values there is a clear trend with coarsening resolution. If DEM resolution increases, critical rainfall values increase to make more cells available for landslide initiating to compensate for lower slope gradients. This is at the cost of stable cell prediction and overall *MSR*. The optimal parameter combinations give no indication that these are the most realistic values or have a clear link with physical properties.

Resampling to coarser resolutions filters out high slope gradients and smoothens the landscape (Table 5). As high slope gradients are an important factor in triggering landslides, this will influence the landslide locations because possible initiation locations are lost and landslide routing becomes less accurate.

Furthermore the total watershed area might be altered by the resampling. Claessens et al. (2005) showed that coarser resolutions yield higher specific catchment areas (contributing area per unit contour length). Effects of resolution on the distribution of slope gradient and specific catchment area have a direct impact on critical rainfall calculations (Claessens et al., 2005).

At 10 m resolution the model does not perform satisfactory any more for our small-scale catchment. This is in contrast to the findings of Keijsers et al. (2011) where the LAPSUS-LS model performed

Table 4
MSR for different DEM resolutions.

DEM resolution (m)	*MSR* (−)	Landslide prediction	Stable cell prediction	C (−)	φ (°)	T ($m^2\ d^{-1}$)	ρ_s ($g\ cm^{-3}$)	Rainfall intensity
1	0.851	0.897	0.806	0.1	30.4	15	1.8	0.01
2	0.775	0.724	0.826	0.1	34.4	18	1.8	0.03
5	0.709	0.828	0.590	0.1	29.4	13	1.5	0.05
10	0.568	0.538	0.598	0.1	29.4	10	1.5	0.1

Table 5
Hinenui study area minimum, maximum, mean and standard deviation of slope gradients in relation to DEM resolution.

DEM resolution (m)	Min (°)	Max (°)	Mean (°)	SD
1	0.01	56.67	21.40	10.16
2	0.13	44.66	21.03	9.83
5	0.65	40.23	20.06	9.19
10	1.34	36.46	18.63	8.39

satisfactory with 9 m resolution. In this study the 10 m resolution itself might not be the cause of the low success in predicting landslides. Rather the aggregation method affected slope characteristics and contributing area. In other words, this small-scale landscape with rather short slope lengths is very sensitive for the grid cell resolution and number of grids in the downslope direction (Schoorl et al., 2000). In addition, Claessens et al. (2005) stress that topographical and hydrological properties do vary for different landscapes and that optimal DEM resolution is thus context-dependent. Large watersheds with long slope lengths may perform better with coarser resolutions than small watersheds with short slopes. Taking into consideration earlier arguments that more complex and localised processes play a role in landsliding in this small catchment, finer resolutions might capture those processes better.

5. Conclusions

LAPSUS-LS, the landslide component of a multi-dimensional landscape evolution model, combines a steady-state hydrological model with an infinite slope model to predict the triggering of landslides and their subsequent movement downslope. The performance of the model has been studied with an existing dataset of 71 mapped shallow landslides in the Hinenui catchment on the East Coast of North Island, New Zealand. The performance of the model was optimised by calibrating parameter values for topographical, hydrological and geotechnical terrain attributes. The highest *MSR* value for the study area (0.851) was achieved at 1 m resolution for a specific parameter combination.

Landslides located upslope were generally not well predicted, and there was an over-prediction of landslides in local drainage channels. This discrepancy could be due to inaccuracies in the DEM or other input data, lumping of soil and vegetation parameters, due to the possibility that relevant processes for this particular landscape and process context are not included in the model, or due to limited validity of the infinite length assumption for landslides with a small length/depth ratio. The complex geometry of the catchment with different stages of regolith stripping changes both the hydrological and geotechnical conditions of slopes and adds more complexity to the spatial variation of critical rainfall values calculated by the model. Solutions could be to introduce a legacy effect in the model by using multiple time steps, and to introduce spatial variability in soil and vegetation parameters. The specific characteristics of the landslides in the area might make the model performance vulnerable for simplifications regarding steady-state hydrology and rainfall characteristics.

Furthermore, the effect of DEM resolution on model performance was studied. *MSR* decreased with increasing DEM resolution. The trade-off between a correct prediction of landslides versus stable cells becomes increasingly worse with coarser resolutions. Resampling to coarser resolutions filters out high slope gradients and smoothens the landscape. As high slope gradients are an important factor in triggering landslides, this will influence the landslide locations, resulting in the loss of possible initiation locations and less accurate landslide routing. Other variables like total watershed surface area and specific catchment area also change with resolution.

In this environmental context the 1 m resolution topography seems to resemble reality most closely and landslide locations are better distinguished from stable areas than for coarser resolutions. More gain in model performance could be achieved by adding complexities and parameter variations in the catchment. This is an interesting topic for further research. However, at this moment the model performs satisfactory at the 1 m resolution in the sense that it can give a reliable indication of spatial distribution of landslide hazard and can potentially be used in hazard mitigation and disaster prevention.

Acknowledgements

In memoriam of Dr. Nicholas J. Preston (1965–2010) who kindly permitted the use of his Hinenui sediment delivery ratio dataset for this research paper to allow continued research in geomorphology. The digitisation of the Hinenui dataset was funded by the Terrestrial Landscape Change: MARGINS Source-to-Sink New Zealand Programme under contract number C05X0705.

References

Barling, D.B., Moore, I.D., Grayson, R.B., 1994. A quasi-dynamic wetness index for characterizing the spatial distribution of zones of surface saturation and soil water content. Water Resources Research 30, 1029–1044.
Borga, M., Dalla Fontana, G., Da Ros, D., Marchi, L., 1998. Shallow landslide hazard assessment using a physically based model and digital elevation data. Environmental Geology 35, 81–88.
Borga, M., Dalla Fontana, G., Gregoretti, C., Marchi, L., 2002a. Assessment of shallow landsliding by using a physically based model of hill slope stability. Hydrological Processes 16, 2833–2851.
Borga, M., Dalla Fontana, G., Cazorzi, F., 2002b. Analysis of rainfall-triggered shallow landsliding using a quasi-dynamic wetness index. Journal of Hydrology 268, 56–71.
Brooks, S.M., Crozier, M.J., Preston, N.J., Anderson, M.G., 2002. Regolith stripping and the control of shallow translational hill slope failure: application of a two-dimensional coupled soil hydrology-slope stability model, Hawke's Bay, New Zealand. Geomorphology 45, 165–179.
Burton, A., Bathurst, J.C., 1998. Physically based modeling of shallow landslide sediment yield at a catchment scale. Environmental Geology 35, 89–99.
Chiang, S.H., Chang, K.T., 2009. Application of radar data to modeling rainfall-induced landslides. Geomorphology 103, 299–309.
Claessens, L., Heuvelink, G.B.M., Schoorl, J.M., Veldkamp, A., 2005. DEM resolution effects on shallow landslide hazard and soil redistribution modelling. Earth Surface Processes and Landforms 30, 461–477.
Claessens, L., Lowe, D.J., Hayward, B.W., Schaap, B.F., Schoorl, J.M., Veldkamp, A., 2006. Reconstructing high-magnitude/low-frequency landslide events based on soil redistribution modelling and a Late-Holocene sediment record from New Zealand. Geomorphology 74, 29–49.
Claessens, L., Schoorl, J.M., Veldkamp, A., 2007a. Modelling the location of shallow landslides and their effects on landscape dynamics in large watersheds: an application for Northern New Zealand. Geomorphology 87, 16–27.
Claessens, L., Knapen, A., Kitutu, M.G., Poesen, J., Deckers, J.A., 2007b. Modeling landslide hazard, soil redistribution and sediment yield of landslides on the Ugandan footslopes of Mount Elgon. Geomorphology 90, 23–35.
Crozier, M.J., 1986. Landslides: Causes, Consequences and Environment. Croom Helm, London.
Crozier, M.J., Preston, N.J., 1999. Modelling changes in terrain resistance as a component of landform evolution in unstable hill country. Process Modelling and Landform Evolution 78, 267–284.
Hewitt, K., Clague, J.J., Orwin, J.F., 2008. Legacies of catastrophic rock slope failures in mountain landscapes. Earth-Science Reviews 87, 1–38.
Huang, J.C., Kao, S.J., 2006. Optimal estimator for measuring landslide model efficiency. Hydrology and Earth System Sciences 10, 957–965.
Iverson, R.M., 2000. Landslide triggering by rain infiltration. Water Resources Research 36, 1897–1910.
Johnson, A.M., Rodine, J.R., 1984. Debris flow. In: Brunsden, D., Prior, D.B. (Eds.), Slope Instability. Wiley, Chicester, pp. 257–361.
Jones, K.E., 2009. Contemporary Sediment Delivery Ratios for Small Catchments Subject to Shallow Rainfall Triggered Earthflows in the Waipaoa Catchment, North Island, New Zealand. Msc Thesis, School of Geography, Environment and Earth Sciences Victoria University of Wellington.
Jones, J.A.A., 2010. Soil piping and catchment response. Hydrological Processes 24, 1548–1566.
Keijsers, J.G.S., Schoorl, J.M., Chang, K.-T., Chiang, S.-H., Claessens, L., Veldkamp, A., 2011. Calibration and resolution effects on model performance for predicting shallow landslide locations in Taiwan. Geomorphology 133, 168–177.
Mazengarb, C., Speden, I.G. 2000: Geology of the Raukumara area: scale 1:250,000. Institute of Geological and Nuclear Sciences 1:250,000 geological map 6. 60 p. + 1 fold. Map.

Milledge, D.G., Griffiths, D.V., Lane, S.N., Warburton, J., 2012. Limits on the validity of infinite length assumptions for modelling shallow landslides. Earth Surface Processes and Landforms 37, 1158–1166.
Montgomery, D.R., Dietrich, W.E., 1994. A physically based model for the topographic control on shallow landsliding. Water Resources Research 30, 1153–1171.
Moore, I.D., O'Loughlin, E.M., Burch, G.J., 1988. A contour based topographic model for hydrological and ecological applications. Earth Surface Processes and Landforms 13, 305–320.
O'Loughlin, E.M., 1986. Prediction of surface saturation zones in natural catchments by topographic analysis. Water Resources Research 22, 794–804.
Pack, R.T., Tarboton, D.G., Goodwin, C.N., 2001. Assessing terrain stability in a GIS using SINMAP. 15th Annual GIS Conference, 19–22/02/2001, Vancouver, British Columbia.
Preston, N.J., 1996. Spatial and temporal changes in terrain resistance to shallow transitional regolith landsliding. MA (Hons) thesis, Victoria University of Wellington, Wellington, New Zealand.
Preston, N.J., 2008. Off-slope sediment delivery from landsliding during a storm, Muriwai Hills, North Island, New Zealand. Sediment dynamics in changing environments, proceedings of a symposium held in Christchurch, New Zealand. IAHS Publication 325, 237–241.
Quinn, P., Beven, K., Chevallier, P., Planchon, O., 1991. The prediction of hill slope flow paths for distributed hydrological modelling using digital terrain models. Hydrological Processes 5, 59–79.
Reid, L.M., Page, M.J., 2002. Magnitude and frequency of landsliding in a large New Zealand catchment. Geomorphology 49, 71–88.
Schoorl, J.M., Sonneveld, M.P.W., Veldkamp, A., 2000. Three-dimensional landscape process modelling: the effect of DEM resolution. Earth Surface Processes and Landforms 25, 1025–1043.
Tarolli, P., Fontana, G.D., 2009. Hillslope-to-valley transition morphology: new opportunities from high resolution DTMs. Geomorphology 113, 47–56.
Tarolli, P., Tarboton, D.G., 2006. A new method for determination of most likely landslide initiation points and the evaluation of digital terrain model scale in terrain stability mapping. Hydrology and Earth System Sciences 10, 663–677.
Trustrum, N.A., Thomas, V.J., Lambert, M.G., 1984. Soil slip erosion as a constraint to hill country pasture production. Proceedings of the New Zealand Grasslands Association 45, 57–64.
Zhang, W., Montgomery, D.R., 1994. Digital elevation model grid size, landscape representation, and hydrologic simulations. Water Resources Research 30, 1019–1028.